

Arrangement dependence of interparticle force in nematic colloids

Takahiro Kishita,¹ Kenji Takahashi,¹ Masatoshi Ichikawa,^{1,*} Jun-ichi Fukuda,^{2,†} and Yasuyuki Kimura^{1,‡}
¹*Department of Physics, School of Sciences, Kyushu University, 6-10-1 Hakozaki, Higashi-ku, Fukuoka 812-8581, Japan*
²*Nanotechnology Research Institute, AIST, 1-1-1 Umezono, Tsukuba 305-8568, Japan*

(Received 19 October 2009; published 7 January 2010)

We have experimentally and theoretically studied the interparticle force between two colloidal particles with different sizes accompanied by hyperbolic hedgehog defects in a nematic liquid crystal. The force f was directly measured using dual-beam optical tweezers and calculated theoretically from the equilibrium tensor field around the particles. The dependence of f on the center-to-center distance between particles of different sizes R is different from that for particles with the same size. The magnitude of f depends on the relative arrangement of the particles: f is larger when a defect between the particles belongs to the larger particle. From the theoretical calculation, the difference in f between the two arrangements, δf , monotonically increases with increasing size difference. The difference δf was experimentally and theoretically found to be proportional to $R^{-4.6}$ at large R . The obtained exponent is comparable to the exponent of -5 predicted by electrostatic analogy.

DOI: [10.1103/PhysRevE.81.010701](https://doi.org/10.1103/PhysRevE.81.010701)

PACS number(s): 61.30.Jf, 61.30.Gd, 82.70.Dd

The interaction between colloidal particles in isotropic fluids has been intensively studied from both fundamental viewpoints and for its applications. In particular, van der Waals and electrostatic interactions act over a long distance and are important for the stability of large colloids in isotropic liquids. The magnitudes of these interactions are typically on the order of the thermal energy at a distance of micrometers [1,2]. However, the specific interaction between colloids in structured fluids such as liquid crystals (LCs) and polymers has not been fully studied.

A LC is an anisotropic fluid in which the rotational symmetry is broken. A nematic liquid crystal (NLC) is a typical liquid crystalline phase. In an NLC, the centers of mass of constituent molecules are randomly distributed, but their long axes point in the same direction on average. This direction is represented by a unit vector called a director. The existence of orientational order in a nematic medium induces the characteristic interaction between colloidal particles dispersed in an NLC. The anchoring of the LC at the particle surface deforms the director field, and the particle is subjected to a force from the NLC to minimize the deformation [3–8].

This specific interaction between colloids, mediated by the elasticity of the NLC, depends on the anchoring conditions at the particle surface (strength and direction) and the particle size. In particular, in the case of strong homeotropic surface anchoring, a particle can be regarded as a point defect (radial hedgehog), and an accompanying defect (hyperbolic hedgehog) is spontaneously formed near the particle to conserve the total topological charge and to minimize the free energy of the system [5–8]. This type of a particle-defect pair (see Fig. 1) is often called a *dipole* owing to its shape and its behavior, which is analogous to that of an electric dipole moment.

The dipolar-type interaction between the particles in the particle-defect pair in an NLC has been theoretically predicted using the electrostatic analogy [4,6]. The interparticle force f is proportional to R^{-4} (R is the center-to-center distance between the particles) and f is anisotropic, depending on the angle between the two dipoles. This prediction has been confirmed experimentally [9–14] and by numerical calculations [15–18]. It has also been established that the interaction energy is much larger than those of van der Waals and screened Coulombic interactions at the same distance. For example, the attractive interaction energy between two colinearly aligned dipoles is as large as a few thousand $k_B T$ (k_B is the Boltzmann constant and T is the absolute temperature) at several microns [12–14].

Recently, we have reported some complex regular structures that are formed upon the phase separation of an NLC and polymer mixture [19]. In this phase-separation process, the size distribution of the polymer droplets is one of the origins of the variety of self-assembled structures. The interparticle force between particles with different sizes is qualitatively different from that between particles with the same size. This feature is important in understanding the mechanism of the formation of these complex structures when designing the desired microstructure in an NLC. Although some studies on the interparticle force in an NLC have been reported, they were limited to the force between particles

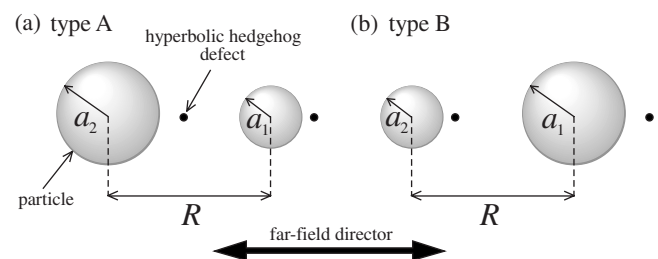


FIG. 1. Possible arrangements of two particles with different sizes. (a) Type A: the larger particle is on the left side ($a_2 > a_1$). (b) Type B: the smaller particle is on the left side ($a_2 < a_1$). The two particles (dipoles) are aligned parallel to the far-field director.

*Present address: Department of Physics, Kyoto University, Kyoto 606-8502, Japan; ichi@scphys.kyoto-u.ac.jp

†fukuda.jun-ichi@aist.go.jp

‡kimura@phys.kyushu-u.ac.jp

with the same sizes with some exceptions [6,11,18,20].

According to the electrostatic analogy of nematic colloids discussed by Lubensky *et al.* [6], the dependence of f on R for two particles with radii a_1 and a_2 , as shown in Fig. 1, is given by

$$\frac{f}{4\pi K} = -\frac{6\alpha^2 a_1^2 a_2^2}{R^4} + \frac{24\alpha\beta a_1^2 a_2^2 (a_1 - a_2)}{R^5} + \frac{120\beta^2 a_1^3 a_2^3}{R^6}, \quad (1)$$

where K is the elastic constant of the NLC (one-constant approximation), α is the dipolar constant ($\alpha=2.04$), and β is the quadrupolar constant ($\beta=0.72$). The second term on the right-hand side of Eq. (1) (dipole-quadrupole term) appears only for $a_1 \neq a_2$, and its sign depends on the relative arrangement of the particles. The attractive force is expected to be larger in the case of Fig. 1(a) than in the case of Fig. 1(b) at the same R . Another property predicted by Eq. (1) is that the difference between the forces in the two arrangements, δf , should be proportional to R^{-5} .

The purpose of this Rapid Communication is to study the arrangement dependence of the interparticle force between different-sized particles in an NLC, both experimentally using optical tweezers and theoretically by numerical calculation.

In experiments, we used dual-beam optical tweezers to trap two particles with different sizes. One beam is fixed, and the interparticle force f is evaluated from the displacement of the trapped particle by the fixed beam [13,14]. The distance R is varied along the direction parallel to the far-field director by scanning the other beam as slowly as 50 nm/s.

Polystyrene latex particles with radii of 2.55 and 2.0 μm (Magsphere Inc.) were used as colloidal particles. Their surfaces were coated with octadecyldimethyl (3-trimethoxysilylpropyl) ammonium chloride (DMAOP) to promote the homeotropic anchoring of the LC. For the stable trapping of particles in an NLC using the optical tweezers, they were dispersed in an NLC with a low refractive index (MJ032358, Merck Japan) [21]. To avoid the effect of surface screening [22,23], we used a cell with the thickness of over 20 μm .

Figure 2(a) shows the dependence of f on R for the type A and B arrangements. A negative value of f represents an attractive force and a positive value represents a repulsive force. In both arrangements, f is attractive at large R and repulsive at small R . Such a behavior is qualitatively similar to that observed for particles with the same size [11,13,14]. At the distance where $f=0$, $R_{f=0}$, the particles form a stable pair without direct contact. $R_{f=0}$ is, respectively, about 5.4 and 5.3 μm for the type A and B arrangements. These values are almost 1.2 in the reduced scale $R_{f=0}/(a_1+a_2)$. For equal-sized particles, the stable position ($f=0$) is reported to be about $1.2 \times 2a$ (a is the radius of a particle) [5–7,11,13,15]. At large R , the magnitude of the attractive force in the type A arrangement is larger than that in the type B arrangement. The minimal values of f (the maximum values of the magnitude) for arrangement types A and B are, respectively, -30.2 pN at 6.2 μm and -20.5 pN at 6.1 μm . The difference in force between the two arrangements at large R can be qualitatively understood because the distance between the

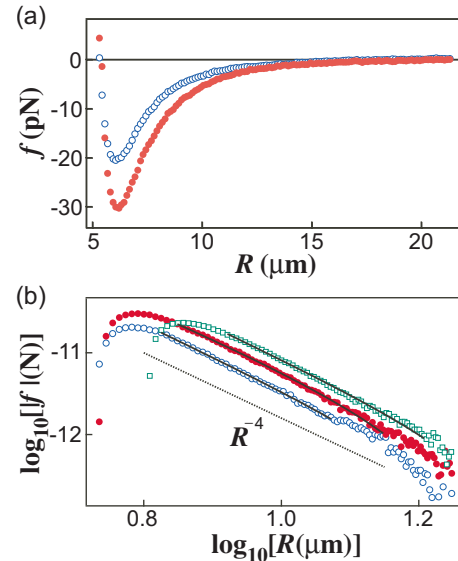


FIG. 2. (Color online) Dependence of the interparticle force f on the center-to-center interparticle distance R for particles with radii of 2.55 and 2.0 μm . The force curves in a logarithmic plot are shown in (b). Filled circles (red online): type A. Empty circles (blue online): type B. Empty squares (green online): particles with the same size (radius of 2.55 μm). The solid lines in (b) are the best fits to experimental data using Eq. (1). The dotted line in (b) shows R^{-4} dependence as a guide to the eye.

sandwiched defect and the surface of the other (nonpairing) particle is shorter for the type A arrangement.

The force f between the particles with the same size has been confirmed experimentally to be proportional to R^{-4} at large R [9–11,13,14]. However, at large R , the force between particles with different sizes has a stronger dependence on R as shown in Fig. 2(b). Noël *et al.* [11] analyzed the interparticle force between particles with slightly different sizes using Eq. (1) and determined the contribution of the higher-order multipolar components. We also analyzed the dependence of f on R using Eq. (1) for both types of arrangement. The best-fitted curves obtained using Eq. (1) are drawn as solid lines in Fig. 2(b). In the fitting procedure, the average of the measured splay and bend elastic constants, $\bar{K} = 6$ pN, was used as the elastic constant K . The best-fitted values are $\alpha = 2.38 \pm 0.02$ and $\beta = 0.74 \pm 0.05$ for the type A arrangement and $\alpha = 1.77 \pm 0.03$ and $\beta = 0.09 \pm 0.9$ for type B. For the equal-sized particles, we obtained $\alpha = 2.21 \pm 0.04$ and $\beta = 0.497 \pm 0.09$ by fitting the data to Eq. (1), disregarding the second term. Although the obtained values of α are approximately 2 and are comparable to those utilized in the electrostatic analogy, the values of β are considerably different for each arrangement. This is due to the arbitrariness of the range of data to which the regression analysis was applied. Only the asymmetric term can be extracted with better accuracy, as will be discussed later.

The interparticle force between different-sized particles was also studied by numerical calculation in this study. Numerical studies on the interparticle force between particles with the same size in a dipole configuration have been reported [15–18]. Among them, the theoretical force curves

obtained by the method developed by Fukuda *et al.* [15,16] are in good agreement with our previous experimental results for particles with the same size [13]. In the present study, the method of Fukuda *et al.* was extended to the case of two particles with different sizes, and the dependence of f on R was calculated. Since the detail of the calculation has already been published [15,16], only its outline will be reviewed below.

First, the equilibrium profile of a nematic field around two particles was calculated for a given interparticle distance D by minimizing the reduced free energy \bar{F} , written in terms of a second-rank-tensor order parameter Q [15,16] as

$$\bar{F} = \int_{\Omega} dr \left[\frac{\tau}{2} \text{Tr} Q^2 - \frac{\sqrt{6}}{4} \text{Tr} Q^3 + \frac{1}{4} (\text{Tr} Q^2)^2 + \frac{\xi_R^2}{2} \partial_k Q_{ij} \partial_k Q_{ij} \right], \quad (2)$$

where τ ($=-5.4 \times 10^{-2}$) is the reduced temperature, ξ_R ($=5 \times 10^{-3}a$) is the coherence length of the nematic host, and Ω is the region occupied by the NLC outside the two particles. In the following calculation, the length is reduced by the radius of the larger particle a (for example, $D=R/a$). The system has normal boundary conditions at the particle surfaces, and a uniform alignment parallel to the z axis is assumed far from the particles.

In the calculation, we adopted the modified version of bispherical coordinates with an “adaptive mesh” [24], which is applicable to two particles with different radii. Using this coordinate system, the equilibrium tensor field Q around the particles was obtained by relaxing the free energy \bar{F} using the simple equation of motion $\partial Q_{ij} / \partial t = -\Gamma (\delta \bar{F} / \delta Q_{ij} + \lambda \delta_{ij})$, where Γ is the kinetic coefficient and λ is the Lagrange multiplier used to ensure that $\text{Tr} Q = 0$. From the value of Q obtained in equilibrium, the force \bar{f} subjected to a particle from the nematic field was calculated by integrating the stress tensor over the surface enclosing the particle [16].

The dependence of the dimensionless interparticle force \bar{f} on D , obtained numerically for pairs of particles with different sizes, is shown in Fig. 3. The force curves for four different particle ratios, 1:1, 1:0.9, 1:0.8, and 1:0.7, are shown for both arrangements. In the case of a much larger size difference, the dipolar configuration tends to be unstable, and the transition to the Saturn-ring configuration is observed with decreasing D . In such cases, the interparticle force is markedly lower than that between dipoles, as reported in Refs. [25,26]. Therefore, only the force curves for the particles with a hyperbolic hedgehog at each distance D considered are shown in Fig. 3.

Similarly to our experimental results, the magnitude of the attractive force in the type A arrangement is larger than that in the type B arrangement for the same size ratio. In both arrangements, the magnitude of the attractive force at large D monotonically decreases with increasing difference in size. This can be understood from the electrostatic analogy. The main contribution to \bar{f} is from the first term of Eq. (1), and its magnitude decreases with increasing difference in size. The difference between the two arrangements is due to

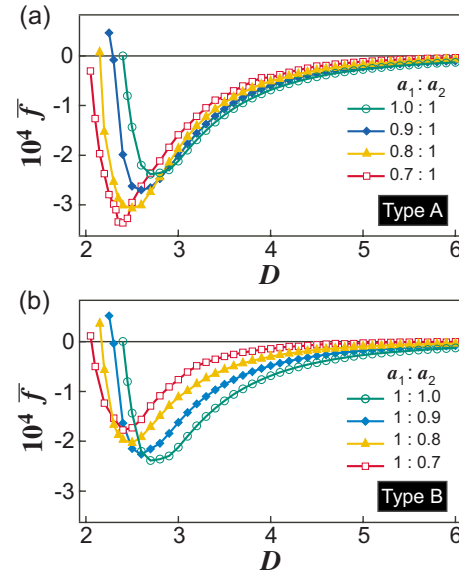


FIG. 3. (Color online) Dependence of dimensionless interparticle force \bar{f} on the reduced interparticle distance D . (a) Particles in type A arrangement ($a_1 \leq a_2$). (b) Particles in type B arrangement ($a_1 \geq a_2$).

the contribution of the second term of Eq. (1). The rate of decrease in magnitude is smaller in the type A arrangement because the second term is negative for type A and positive for type B. Therefore, the difference between \bar{f} for the two arrangements monotonically increases with increasing size difference. The maximum magnitude of the attractive force increases with increasing size difference for type A but decreases for type B. Such a behavior at small D cannot be understood by considering the electrostatic analogy. This is probably due to the fact that the repulsive force between particles is smaller for a pair with a large size difference.

The force curves obtained experimentally and theoretically are directly compared in Fig. 4. In the figure, the magnitude of f obtained by theoretical calculation is adjusted to fit the experimental data for type A. The only parameter that requires adjustment to fit the experimental and theoretical results is the magnitude of the force curve. For both arrangements and for particles with equal size, the profiles of the theoretical and experimental force curves are in good agreement. To the best of our knowledge, the direct comparison between the experimental and simulated force curves has not

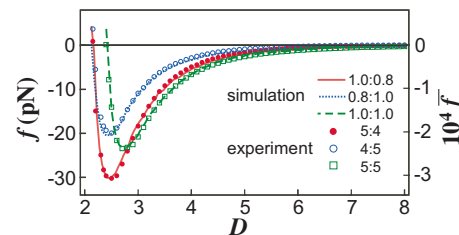


FIG. 4. (Color online) Comparison between experimentally obtained force curves and theoretical calculations. The calculated force curves are scaled to fit the experimental result for type A arrangement (filled circles).

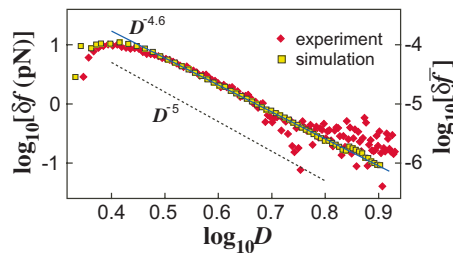


FIG. 5. (Color online) Dependence of the difference in the interparticle force between the two arrangements δf on the reduced interparticle distance D . The dotted line (black online) is proportional to D^{-5} , which is expected from the electrostatic analogy. The best-fitted slope to the theoretical calculation, drawn as a thick line (blue online), is proportional to $D^{-4.6}$.

been reported before. Their agreement shows the reliability of both methods utilized in this study.

To discuss the difference in f between the type A and B arrangements, δf , both experimental and theoretical values are plotted with a logarithmic scale in Fig. 5. The dependences of δf on D obtained experimentally and theoretically are in good agreement. The dependence $\delta f \propto D^{-5}$ is also drawn as a dotted line, which is predicted using Eq. (1). Although the dependence of δf on D has a slightly different exponent of -4.60 ± 0.02 at large R , the electrostatic analogy

also appears to be applicable to particles of different sizes at large D .

We have experimentally and theoretically studied the interparticle force f between particles with different sizes in an NLC. The two different arrangements of different-sized dipoles exhibit characteristic force profiles due to the difference in the particle sizes. The numerical calculation well explains the experimental results semiquantitatively. The asymmetric term of R^{-5} predicted using the electrostatic analogy is slightly different from the results for both arrangements. The asymmetric interparticle force in an NLC reported in this Rapid Communication originates from the asymmetric form of dipolar-type colloidal-defect pairs. This type of asymmetric force is expected to be useful for manufacturing specific self-assembled patterns of colloids in an NLC. An example of a self-assembled structure fabricated by phase separation has been reported [19,27]. In such a self-assembly process, the anisotropic and asymmetric interparticle force causes the structures to form uniformly, despite the nematic field being uniaxial.

The authors thank Dr. A. Sawada at Merck Japan, Ltd., for providing the liquid crystal sample. This work was supported by a Grant-in-Aid for Scientific Research on Priority Area “Soft Matter Physics” from MEXT, Japan. Y.K. and M.I. were also supported by a Grant-in-Aid for Scientific Research from JSPS.

- [1] W. B. Russel, D. A. Saville, and W. R. Schowalter, *Colloidal Dispersions* (Cambridge University Press, Cambridge, England, 1989).
- [2] J. N. Israelachvili, *Intermolecular and Surface Forces* (Academic, London, 1992).
- [3] E. M. Terentjev, *Phys. Rev. E* **51**, 1330 (1995).
- [4] P. Poulin, H. Stark, T. C. Lubensky, and D. A. Weitz, *Science* **275**, 1770 (1997).
- [5] P. Poulin and D. A. Weitz, *Phys. Rev. E* **57**, 626 (1998).
- [6] T. C. Lubensky, D. Pettey, N. Currier, and H. Stark, *Phys. Rev. E* **57**, 610 (1998).
- [7] H. Stark, *Phys. Rep.* **351**, 387 (2001).
- [8] J.-I. Fukuda, *J. Phys. Soc. Jpn.* **78**, 041003 (2009).
- [9] P. Poulin, V. Cabuil, and D. A. Weitz, *Phys. Rev. Lett.* **79**, 4862 (1997).
- [10] M. Yada, J. Yamamoto, and H. Yokoyama, *Phys. Rev. Lett.* **92**, 185501 (2004).
- [11] C. M. Noël, G. Bossis, A.-M. Chaze, F. Giulieri, and S. Laci, *Phys. Rev. Lett.* **96**, 217801 (2006).
- [12] M. Škarabot, M. Ravnik, S. Žumer, U. Tkalec, I. Poberaj, D. Babič, N. Osterman, and I. Muševič, *Phys. Rev. E* **76**, 051406 (2007).
- [13] K. Takahashi, M. Ichikawa, and Y. Kimura, *Phys. Rev. E* **77**, 020703(R) (2008).
- [14] K. Takahashi, M. Ichikawa, and Y. Kimura, *J. Phys.: Condens. Matter* **20**, 075106 (2008).
- [15] J.-I. Fukuda, H. Stark, M. Yoneya, and H. Yokoyama, *Phys. Rev. E* **69**, 041706 (2004).
- [16] J.-I. Fukuda, H. Stark, M. Yoneya, and H. Yokoyama, *Mol. Cryst. Liq. Cryst.* **435**, 63 (2005).
- [17] C. Zhou, P. Yue, and J. J. Feng, *Langmuir* **24**, 3099 (2008).
- [18] K. S. Korolev and D. R. Nelson, *Phys. Rev. E* **77**, 051702 (2008).
- [19] K. Kita, M. Ichikawa, and Y. Kimura, *Phys. Rev. E* **77**, 041702 (2008).
- [20] M. Škarabot, M. Ravnik, S. Žumer, U. Tkalec, I. Poberaj, D. Babič, and I. Muševič, *Phys. Rev. E* **77**, 061706 (2008).
- [21] The extraordinary and ordinary refractive indices of MJ032358 are $n_e=1.5$ and $n_o=1.46$, respectively. The refractive index of a polystyrene particle is 1.6.
- [22] M. Vilfan, N. Osterman, M. Čopič, M. Ravnik, S. Žumer, J. Kotar, D. Babič, and I. Poberaj, *Phys. Rev. Lett.* **101**, 237801 (2008).
- [23] J.-I. Fukuda and S. Žumer, *Phys. Rev. E* **79**, 041703 (2009).
- [24] J. Fukuda and H. Yokoyama, *Eur. Phys. J. E* **4**, 389 (2001).
- [25] I. I. Smalyukh, O. D. Lavrentovich, A. N. Kuzmin, A. V. Kachynski, and P. N. Prasad, *Phys. Rev. Lett.* **95**, 157801 (2005).
- [26] J. Kotar, M. Vilfan, N. Osterman, D. Babič, M. Čopič, and I. Poberaj, *Phys. Rev. Lett.* **96**, 207801 (2006).
- [27] J.-C. Loudet, P. Barois, and P. Poulin, *Nature (London)* **407**, 611 (2000).